Combustion and Flame 218 (2020) 19–26

Contents lists available at ScienceDirect

Combustion and Flame

journal homepage: www.elsevier.com/locate/combustflame

Autoignition studies of NH_3/CH_4 mixtures at high pressure

Liming Dai[a], Sander Gersen[b], Peter Glarborg[c], Anatoli Mokhov[a], Howard Levinsky[a,*]

[a] Energy and Sustainability Research Institute, University of Groningen, Nijenborgh 6, 9747 AG Groningen, the Netherlands
[b] DNV GL Oil & Gas, P.O. Box 2029, 9704 CA Groningen, the Netherlands
[c] Department of Chemical and Biochemical Engineering, Technical University of Denmark, Kgs. Lyngby DK-2800, Denmark

ARTICLE INFO

Article history:
Received 9 November 2019
Revised 21 April 2020
Accepted 22 April 2020
Available online 7 May 2020

Keywords:
Ammonia ignition
Ammonia/methane mixtures
Ignition enhancement
Oxidation mechanism
RCM measurements

ABSTRACT

Autoignition delay times of NH_3/CH_4 mixtures with CH_4 fractions of 0%, 5%, 10% and 50% were measured in a rapid compression machine at equivalence ratio $\varphi = 0.5$, pressures from 20 to 70 bar and temperatures from 930 to 1140 K. In addition, measurements were performed for NH_3 mixtures with 10% CH_4 at $\varphi = 1.0$ and 2.0. Methane shows a strong ignition-enhancing effect on NH_3, which levels off at higher CH_4 fractions, as the ignition delay time approaches that of pure methane. Autoignition delay times at 10% CH_4 at $\varphi = 0.5$ and 1.0 are indistinguishable, while an increase of ignition delay times by factor of 1.5 was observed upon increasing φ to 2.0. The experimental data were used to evaluate six NH_3 oxidation mechanisms capable of simulating NH_3/CH_4 mixtures. The mechanism previously used by the authors shows the best performance: generally, it predicts the measured ignition delay times to better than 30% for all conditions, except for 50% CH_4 addition for which the differences increase up to 50% at the highest temperature. Sensitivity analysis based on the mechanism used indicates that under lean conditions the reaction $CH_4 + NH_2 = CH_3 + NH_3$ significantly promotes ignition for modest CH_4 addition (5% and 10%), but becomes modestly ignition-inhibiting at 50% CH_4. Sensitivity and rate-of-production analyses indicate that the ignition-enhancing effect of 50% CH_4 addition is closely related to the formation and decomposition of H_2O_2. Flux analysis for NH_3/CH_4 mixtures indicates that $CH_4 + NH_2 = CH_3 + NH_3$ contributes substantially to the decomposition of methane early in the oxidation process, while $CH_3 + NO_2 (+M) = CH_3NO_2 (+M)$ is a significant reservoir of NO_2 at low temperature. Additionally, an anomalous pre-ignition pressure rise phenomenon, which is not reproduced by the simulations, was observed with high reproducibility for the NH_3 mixture with 50% CH_4 addition.

1. Introduction

Ammonia (NH_3) is considered as a promising alternative fuel to replace traditional hydrocarbon fuels in the future. Ammonia can be produced from hydrogen (H_2) and nitrogen (N_2) using sources of renewable electricity such as solar and wind power [1,2]; having a hydrogen density in the liquid form that is higher than liquid hydrogen [3], it is interesting as a potential "carrier" for H_2 as a transportation fuel. At the point of end use, NH_3 can either be converted back to H_2 for fuel-cell vehicles or utilized without conversion in solid oxide fuel cells [4,5]. Alternatively, NH_3 can be used directly in combustion systems to replace hydrocarbon fuels [6,7]. Reiter and Kong [8] demonstrated that by introducing ammonia into the intake manifold and injecting diesel fuel directly into the cylinder to ignite the mixture, ammonia can be used in compression-ignition engine to reduce greenhouse gas emissions. They recommended direct ammonia/diesel injection strategies to increase combustion efficiency and reduce ammonia emissions in the exhaust [9]. One challenge to the use of NH_3 in combustion processes arises from a potential increase in NO_x emission from the nitrogen bound in the fuel [10,11]. Very recently, Okafor et al. [12] and Karuta et al. [6] showed that rich/lean staged combustion could result in low NO_x emissions from an ammonia-fueled micro gas turbine.

Burning velocities of NH_3/air flames have been measured by Takizawa et al. [13] at atmospheric pressure and by Arakawa et al. [14] at pressures from 1 to 5 bar; the results show that the burning velocity of NH_3 is roughly five times lower than that of methane (CH_4). This renders the use of pure ammonia as a fuel particularly challenging for stable and rapid combustion in burners and combustion engines. The use of other fuels as "additives" could enhance the combustion properties to the point at which ammonia can be used with little or no alteration in existing combustion equipment. Following this line of thought, several investigations have been performed to assess the combustion properties

* Corresponding author.
E-mail address: h.b.levinsky@rug.nl (H. Levinsky).

https://doi.org/10.1016/j.combustflame.2020.04.020
0010-2180/

of NH_3 as a pure fuel and blends of NH_3 with other fuels such as hydrogen (H_2) [15–19], diesel [9], dimethyl ether (DME) [10,20], methane (CH_4) [19,21–23] and CO [19].

In addition to increasing the burning rate of ammonia, necessary for the entire range of practical combustion devices, the use of an ammonia/additive mixture in spark- or compression-ignition engines requires the ignition properties of the fuel mixture either to avoid engine knock or, alternatively, to ignite readily. We note that whether the use of a specific additive is fit for a given engine application will depend on the combination of the enhancement of the burning velocity and desired changes ignition properties of the fuel mixture to be used. In addition to measurements of these combustion properties, the ability to model them, using chemical mechanisms demonstrated to reproduce the measurements faithfully, is an essential tool for assessing the potential of fuel/additive mixtures in combustion equipment.

Autoignition delay times have recently been reported of NH_3 [11,24] and NH_3/H_2 mixtures [17,18,25]. Mathieu and Petersen [11] reported shock tube measurements of ignition delay times of highly diluted ammonia mixtures over a wide range of temperature (T = 1560–2455 K), pressure (P, at 1.4, 11, and 30 atm) and equivalence ratio φ = 0.5, 1.0, and 2.0. Shu et al. [24] also performed ignition delay measurements of ammonia in a shock tube at temperatures 1100–1600 K, pressures of 20 and 40 bar, and φ = 0.5, 1.0, and 2.0. More recently, Pochet et al. [17] measured the ignition delay times of NH_3/H_2 mixtures (0, 10 and 25% vol. H_2) under fuel-lean conditions (φ = 0.2, 0.35, 0.5), high pressures (43 and 65 bar) and intermediate temperatures (T = 1000–1100 K) in a rapid compression machine (RCM). He et al. [18] reported the ignition delay times of NH_3 and NH_3/H_2 mixtures (1–20% vol. H_2) measured in an RCM at pressures from 20 to 60 bar, temperatures from 950 to 1150 K, and equivalence ratios from 0.5 to 2. The RCM measurements of ignition delay time by Dai et al. [25] also examined NH_3 and NH_3/H_2 mixtures; pure ammonia was studied for the ranges T = 1040–1210 K, P = 20–75 bar and φ = 0.5–3.0, while NH_3/H_2 mixtures with H_2 fractions from 0 to 10% were studied at equivalence ratios of 0.5 and 1.0. The studies show that pure ammonia has relatively long ignition delay times and that hydrogen addition decreases the ignition delay time substantially.

A potential method to improve the combustion properties of ammonia to facilitate its use as a replacement fuel for natural gas is by the addition of CH_4. Using biomethane for this purpose maintains the renewable nature of the fuel; if only modest quantities of methane as an additive achieve the desired result, using fossil natural gas for this purpose still results in significant reduction in the carbon intensity of the fuel. Focusing on ignition behavior, since natural gas has a high knock resistance in spark-ignited engines, it is important that the autoignition behavior of the resultant mixture [26] does not compromise, and preferably improves, this performance aspect. Assessing the impact of the admixture of methane to ammonia on autoignition requires understanding the oxidation chemistry of the mixed fuel. Given the importance of $-NH_x$ functional groups in the formation of NO from fuel-bound nitrogen, as well the use of ammonia in selective non-catalytic reduction of NO in hydrocarbon-fueled combustion systems, a substantial literature exists regarding the oxidation of NH_3/CH_4 mixtures. For example, studies in flames [21,27,28] and flow reactors [29,30] have been performed to understand the interaction between methane and ammonia in combustion processes.

To our knowledge, no experiments have been performed to measure the ignition delay time of NH_3/CH_4 mixtures under conditions relevant for engine combustion nor have chemical mechanisms describing NH_3/CH_4 autoignition been critically evaluated. To quantify the impact of methane addition to ammonia on autoignition and to provide benchmark data for mechanism evaluation, we report here ignition delay times of NH_3 and NH_3/CH_4 mixtures measured in an RCM, at equivalence ratios of 0.5, 1.0 and 2.0, with CH_4 addition of 0%, 5%, 10% and 50%, pressures in the range 20–70 bar, and temperatures from 930 to 1140 K. Furthermore, we use the measurements to assess the veracity of predictions of ignition using recently developed chemical mechanisms appropriate for ammonia/methane ignition. In addition to the mechanism presented in our previous report on NH_3/H_2 [25], using a modified mechanism from the review on nitrogen chemistry and hydrocarbon/nitrogen interactions by Glarborg et al. [31], five NH_3/CH_4 mechanisms taken from the literature are also evaluated: the mechanism from Shrestha et al. [32], the "San Diego" mechanism [33], from Tian et al. [27], the Li–Konnov mechanism [34] and from Okafor et al. [28]. In addition, a kinetic analysis is performed to provide insight into the changes in ammonia oxidation upon methane addition that are responsible for the ignition behavior of the mixtures.

Table 1
Compositions of NH_3/CH_4 mixtures.

Mixtures	φ	CH_4/fuel	NH_3	CH_4	O_2	N_2	AR
Mixture 1	0.5	0	0.118	0	0.176	0	0.706
Mixture 2	0.5	5%	0.104	0.006	0.178	0	0.712
Mixture 3	0.5	10%	0.098	0.011	0.191	0.105	0.595
Mixture 4	0.5	50%	0.04	0.04	0.22	0.2	0.5
Mixture 5	1.0	10%	0.144	0.016	0.14	0	0.7
Mixture 6	2.0	10%	0.188	0.021	0.091	0	0.7

2. Experiments and simulations

2.1. RCM setup

The ignition delay time measurements were performed in an RCM whose details are described in [35,36] and only a brief description will be given here; salient dimensions of the RCM are included in the Supplemental material. The gas mixtures were compressed in ~10–20 ms to the peak pressure, with 80% of the compression occurring in less than 3 ms. A creviced piston head was used in this machine to obtain a homogenous reacting core during the experiment [37]. The pressure trace is measured by a Kistler ThermoComp quartz pressure sensor with thermal-shock-optimized construction. The temperature after compression (T_c) is obtained by assuming the existence of an adiabatic core, using the following equation, with thermodynamic data from [31]:

$$\int_{T_0}^{T_c} \frac{\gamma(T)}{\gamma(T)-1}\frac{dT}{T} = \ln\left(\frac{P_c}{P_0}\right), \tag{1}$$

where T_0 and P_0 are the initial temperature and pressure, respectively, P_c is the measured pressure after compression and $\gamma(T)$ is the temperature-dependent specific heat ratio of combustible mixture. The compositions (in mole fraction) of the mixtures examined in this study are shown in Table 1. All gas mixtures were prepared in advance in a 10-L gas bottle, used to charge the combustion chamber to the required initial pressure. The mixtures were allowed to mix at least 24 h to ensure homogeneity. To remove any effect of the adsorption of ammonia on the metal surfaces of the facility on the ignition delay time measurements, passivation of the surfaces was done following the procedure proposed by Mathieu and Petersen [11]: the mixing tank and RCM were filled with pure ammonia (10 mbar) for roughly 10 min and then evacuated to 0.7 mbar.

The ignition delay time is defined as the interval between the end of compression and the maximum in the rate of pressure increase during ignition, as illustrated in Fig. 1. The day-to-day reproducibility of the measurements, including repositioning of the piston height, was determined to be better than 5%. (An example

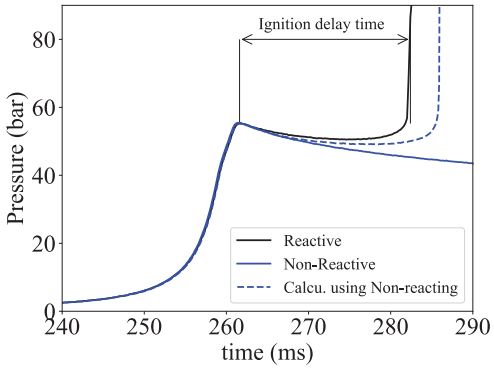

Fig. 1. Pressure traces for mixture 1: measured reactive mixture (black line), equivalent inert mixture (blue line) and simulated reactive mixture (blue dashed line) at $T_c = 1080$ K, $P_c = 55$ bar. (For interpretation of the references to color in this figure, the reader is referred to the web version of this article.)

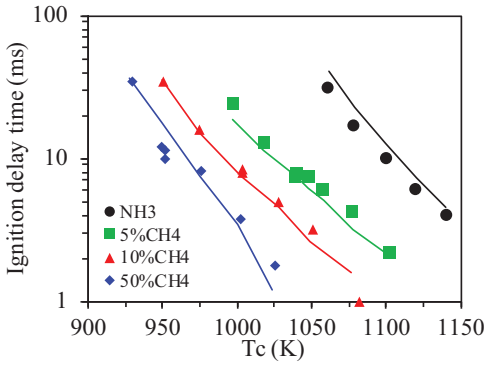

Fig. 2. Measured (symbols) and calculated (lines) ignition delay times of NH_3 as a function of temperature with different CH_4 additions at $\varphi = 0.5$, $P_c = 60$ bar. The data for pure NH_3 are taken from [25]. (Both vertical (±5%) and horizontal (±3.5 K) error bars are not visible in this and other figures). Calculations using the mechanism from [25,31].

of this reproducibility is included in the Supplemental material). The uncertainty of the calculated core gas temperature (T_c) is less than ± 3.5 K for all measurements [38].

2.2. Computational models

The ignition delay time measurements in the RCM were simulated using the homogenous reactor code from Cantera package [39]. To include expansion of the adiabatic core arising from heat loss during the measurements, the specific volume of the adiabatic core is used as input in the simulations. The specific volume is derived from the measured pressure trace of a non-reacting gas mixture that has the same heat capacity as the combustible mixture and used as input into the simulations. An illustration of the measured profile for the combustible and non-reacting mixtures, and of the simulated pressure profile using the non-reacting profile as input, is shown in Fig. 1 for mixture 1 at $T_c = 1080$ K, $P_c = 55$ bar.

2.3. Sensitivity and flux analyses

Sensitivity analyses were performed to identify the most important reactions controlling the autoignition behavior. Sensitivity coefficients (S) were obtained using:

$$S = \frac{(\Delta\tau/\tau)}{(\Delta k_i/k_i)}, \tag{2}$$

where $\Delta\tau$ is the change of ignition delay time corresponding to a change of rate constant Δk_i. A negative coefficient S indicates a promoting effect (reducing ignition delay time when a rate constant is increased) and a positive coefficient denotes an inhibiting effect (increasing ignition delay time when a rate constant is increased). Flux analyses were performed at the point of 20% fuel consumption to study the reaction path under the experimental conditions [40].

3. Results and discussions

3.1. Effect of CH_4 addition at lean conditions

The ignition delay times of NH_3 with CH_4 addition from 0 to 50% were measured at fixed $P_c = 60$ bar and $\varphi = 0.5$, at temperatures ranging from 930 K to 1140 K, as shown Fig. 2. As can be seen, the observed ignition delay times decrease roughly exponentially with increasing temperature at all pressures. The figure illustrates a substantial ignition-enhancing effect of CH_4 addition to NH_3: the ignition delay times of NH_3 are reduced by a factor of ~5 with even a small quantity (5%) of CH_4 at $T_c = 1100$ K. We note that, under the conditions of the experiments, no ignition is observed below ~1050 K for pure ammonia, while methane addition extends the limit of ignition considerably. As seen in Fig. 2, the effect of CH_4 addition decreases at higher CH_4 fraction; the ignition delay times are globally decreased by a factor of ~3 between 5% and 10% methane, and by a factor of ~2 when going from 10% to 50% in the mixture. The calculations, using the mechanism from Glarborg et al. [31] with the modification proposed in [25], predict the measured delay times to better than 30% for 0–10% methane addition; at 50% CH_4, the maximum deviation is ~50%, at $T_c = 1025$ K.

Examining the pressure dependence at fixed temperature, Fig. 3 shows the ignition delay time measurements as function of pressure at $T_c = 1080$ K for 0, 5 and 10% CH_4 (Fig. 3(a)), and at $T_c = 1000$ K for 10% and 50% CH_4 (Fig. 3(b)). The ignition delay times decrease monotonically with increasing pressure for all conditions measured, as also observed for other fuels [35,41], and the curves are more or less parallel. At $T_c = 1080$ K, the ignition delay times of pure NH_3 are reduced by a factor of ~5 by 5% CH_4 addition and reduced by an additional factor of 2 when increasing the methane fraction to 10%. At $T_c = 1000$ K, 50% CH_4 reduces the ignition delay times by another factor of 2.5 as compared to 10% CH_4, also illustrative of the decreasing effect of methane addition at higher methane fraction in the fuel, as observed in Fig. 2. Similar to the data in Fig. 2, for the data in Fig. 3 the mechanism from [25,31] predicts the ignition delay times to within 25% for methane-containing mixtures above ~30 bar, whereas the difference increases to 50% below this pressure.

We note that the data in Fig. 2 for 50% CH_4 in the mixture are within a factor of two of those for pure methane under similar conditions [42,43]; as a result, we did not extend the measurements to higher methane fractions.

Extending the comparison of the measurements with the simulations to the other mechanisms for ammonia/methane ignition indicated above, Fig. 4 shows the comparison of simulations from all 6 mechanisms with the measurements of pure NH_3 at $\varphi = 0.5$, $P_c = 60$ bar taken from Fig. 2, above. In general, the calculations using the mechanism from Tian et al. [27] overpredicts the ignition delay times by more than a factor of 3, while the calculations using the San Diego mechanism [33] agree very well with the measurements. The mechanisms from both Shrestha et al. [32] and Li–Konnov [34] consistently underpredict the measurements by a factor of ~1.5 and ~2, respectively. The mechanism from Okafor et al. [28] fails to predict ignition for pure NH_3 under the conditions in this study.

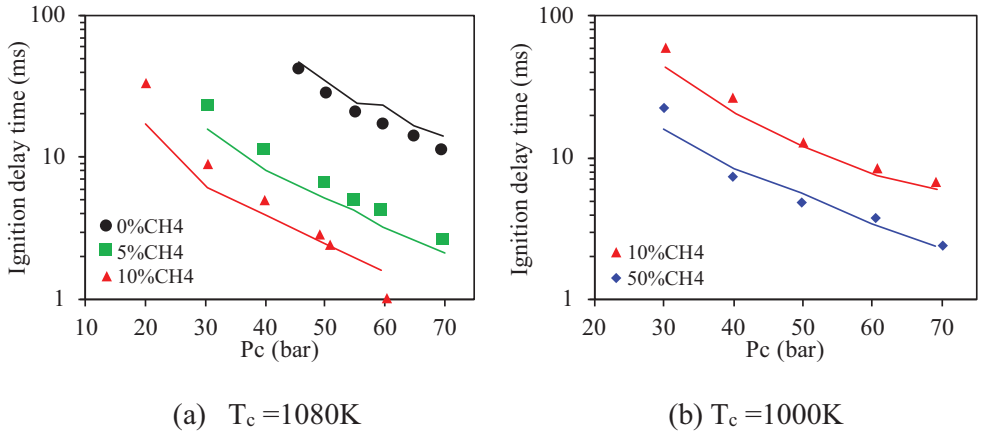

Fig. 3. The measured (symbols) and calculated (lines) ignition delay times as a function of pressure with different CH_4 additions at $\varphi = 0.5$ and fixed $T_c = 1080$ K (a) and $T_c = 1000$ K (b). Calculations using the mechanism from [25,31].

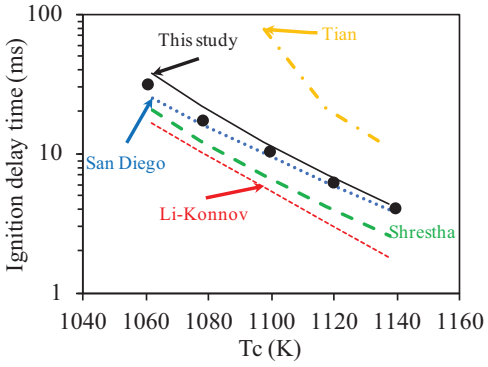

Fig. 4. Measured (symbols) and calculated (lines) ignition delay times of pure NH_3 at $\varphi = 0.5$, $P_c = 60$ bar. Calculations are based on the mechanisms from [25,31] ("This study"), Shrestha et al. [32], "San Diego" [33], Tian et al. [27], Li–Konnov [34] and Okafor et al. [28], respectively.

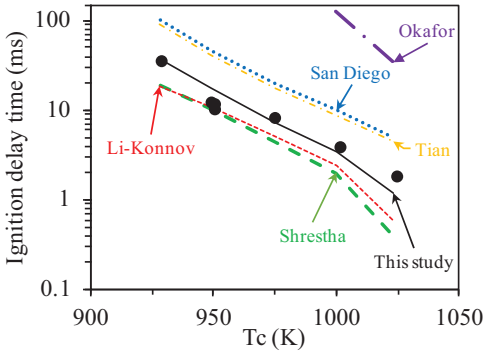

Fig. 5. Measured (symbols) and calculated (lines) ignition delay times of NH_3 with 50% CH_4 at $\varphi = 0.5$, $P_c = 60$ bar. Calculations are based on the mechanisms from [25,31] ("This study"), Shrestha et al. [32], "San Diego" [33], Tian et al. [27], Li–Konnov [34] and Okafor et al. [28], respectively.

The measured ignition delay times of NH_3 with 50% CH_4 taken from Fig. 2 and the calculations using the 6 mechanisms are compared in Fig. 5. Calculations using Tian et al. [27] and the San Diego [33] mechanism both overpredict the ignition delay times by a factor of ~2. The mechanism from Shrestha et al. [32] and the Li–Konnov [34] mechanism both slightly underpredict the ignition delay times, by a factor of ~1.5. While failing to predict any ignition in pure ammonia, the mechanism from Okafor et al. [28] predicts ignition delay times for this NH_3/CH_4 mixture that are too long

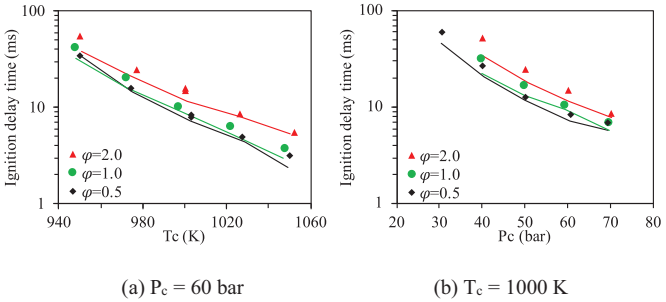

Fig. 6. Ignition delay times of NH_3 with 10% CH_4 addition at $\varphi = 0.5$, 1.0 and 2.0. Symbols are measurements, lines simulations using the mechanism from [25,31] (see text).

by a factor of ~20. Additional comparisons between the full set of measurement data and calculations using the different mechanisms are provided in Supplemental material. Since the mechanism from [25,31] consistently predicts the experimental data well for all mixtures studied here, we only discuss the comparisons with this mechanism below.

3.2. Effect of equivalence ratio

The ignition delay times of NH_3 with 10% CH_4 addition were also measured at $\varphi = 1.0$ and 2.0 as a function of temperature at $P_c = 60$ bar and as a function of pressure at $T_c = 1000$ K, shown in Fig. 6(a) and (b), respectively. As can be seen in both figures, the differences in the ignition delay times at $\varphi = 0.5$ and 1.0 are less than 10%. Increasing φ from 1.0 to 2.0 increases the measured ignition delay times by a factor of ~1.5. Ignition delay times of pure NH_3 at these three equivalence ratios were reported previously in [18,25]; in [25] it was found that ignition delay times of pure NH_3 is increased by a factor of 2 when increasing φ from 0.5 to 1.0 and another factor of 2 when φ is increased from 1.0 to 2.0. Ammonia has longer ignition delay times at higher φ, while the trend is opposite for common hydrocarbon fuels [43,44]. Phenomenologically, the results imply that, upon increasing the equivalence ratio from 0.5 to 1.0, the faster ignition of the hydrocarbon is counteracted by the slower ignition of the ammonia, resulting in no change in the results. Upon increasing φ from 1.0 to 2.0, any potential ignition enhancement from the presence of 10% methane with increasing φ appears to be overwhelmed by the increased delay time from ammonia. The mechanism from [25,31] predicts the ignition delay times very well at all three equivalence ratios, with deviations less

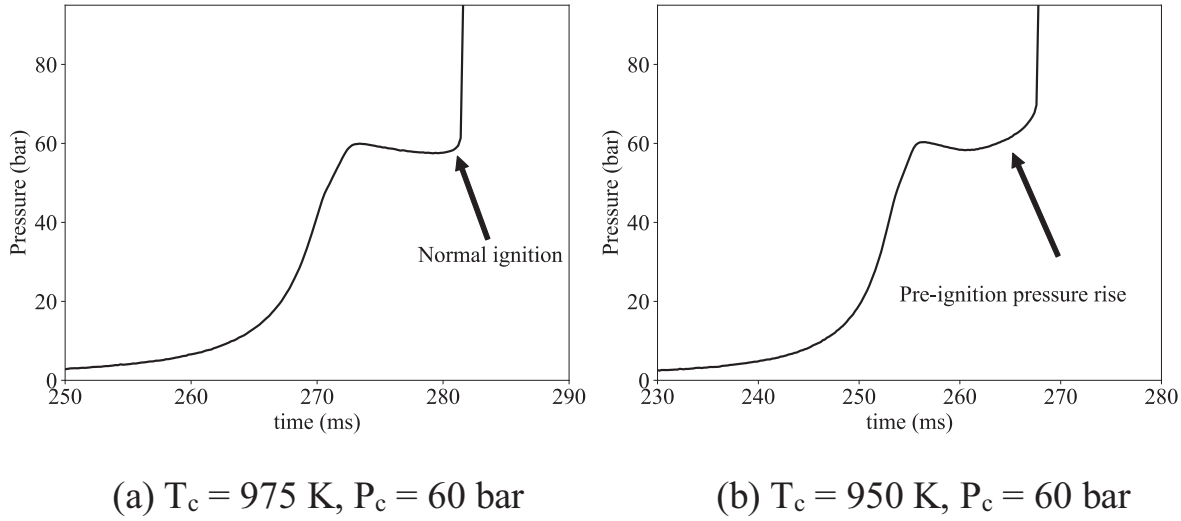

Fig. 7. Pressure traces of normal ignition (a) and anomalous pre-ignition pressure rise (b) observed at 50% CH_4 addition.

than 30% at $\varphi = 0.5$ and 1.0 and with an underprediction of less than 40% at $\varphi = 2.0$.

3.3. Anomalous pre-ignition pressure rise at 50% methane

For the mixture that contains 50% methane in NH_3, an anomalous pre-ignition pressure rise was observed at three conditions (950 K/60 bar, 1000 K/40 bar and 1000 K/50 bar), which resulted in accelerated ignition, similar to that for pure NH_3 reported in [18]. In our experiments, this phenomenon was not observed in other fuel mixtures. Normal ignition is illustrated in Fig. 7(a), in which the pressure rise at ignition is very sharp. In contrast, the pressure trace shown in Fig. 7(b) shows a slow rise over several milliseconds before ignition occurs. Contrary to the reports for NH_3 [18] and ethanol [45], who reported that this phenomenon was irregular, the slow pre-ignition pressure rise observed here was very reproducible: the observed ignition delay time was reproducible to within 2 ms at T_c = 950 K, P_c = 60 bar. This is similar to the results discussed in [46] for ethanol measurements in a shock tube. We point out that the phenomenon reported here resulted in a shortened ignition delay time as compared to the computations, as also noted in [46]; the three points below the simulation line in Fig. 2 at 950 K, and Fig. 3 at 40 and 50 bar are examples of this, while the other experimental points are on or above the simulation line. No simulations (using any of the 6 mechanisms examined) reflected a slow pre-ignition pressure rise. Whether the observed effect arises through the mechanism operative in [46], referred to phenomenologically as “sequential autoignition”, or from some condition-specific chemistry involving the coupling between ammonia and hydrocarbon chemistry not manifest in the current mechanism is a subject of future investigation. However, we do warn that the occurrence of a significant shortening of the ignition delay time could seriously affect the knock resistance of an ammonia/methane fuel adversely in practical engines.

3.4. Kinetic analysis

It will be useful for the discussion of the kinetic aspects of ammonia/methane ignition first to consider the overall oxidation pathways for these mixtures obtained from a flux analysis. This will also expose any interaction between NH_3 and CH_4 during oxidation. A flux analysis was performed for the mixtures studied by tracing both the N (Fig. 8(a)) and C (Fig. 8(b)) elements, at $\varphi = 0.5$, T_c = 1000 K, P_c = 60 bar; as stated above, the flux was analyzed at the point at which 20% of the fuel is consumed. Since the flux analysis for pure ammonia using the same mechanism as applied here has been reported in [25] (albeit at somewhat higher temperature), we focus on the differences in reaction path caused by methane addition. As observed previously [18,24,25], the initial step in ammonia oxidation is to form NH_2, with further oxidation proceeding via either H_2NO or N_2H_4, following reaction of NH_2 with HO_2 or NH_2. At 50% CH_4, while the major oxidation path of NH_3 is unaltered (except that the N_2H_4 channel is suppressed, with a flux lower than 5%), the analysis shows the participation of carbon-containing species as reactants with the nitrogen species. Thus CH_4 and CH_3 become significant in $NH_2 + CH_4 = NH_3 + CH_3$ and $CH_3 + H_2NO = NH_2 + CH_3O$, with the former reaction being the dominant reaction for converting NH_2 back into NH_3. Meanwhile, CH_3NO_2 formation becomes an important route at 50% CH_4 addition. Nitromethane is produced mainly by recombination of CH_3 and NO_2 at low temperatures, but dissociates as the temperature increases. As shown in Fig. 8(b), amine radicals influence the CH_4 oxidation route primarily in the initial stage. CH_4 undergoes H abstraction by NH_2, OH, O and H radicals; the reaction with NH_2 (to produce NH_3 as mentioned above) is second only to oxidation of methane by OH. The methyl radical is mainly oxidized by N-containing species into CH_3O, either directly (by H_2NO and NO_2) or via CH_3OO (by NO). Comparing the paths at 10% CH_4 addition between $\varphi = 0.5$ and $\varphi = 2$ (not shown) indicates little change in the main ammonia routes, but the methane path shifts towards oxidation via ethane following recombination of methyl radicals, as is the case for pure methane. Interestingly, at $\varphi = 2$, $CH_3 + NH_2 (+M) = CH_3NH_2 (+M)$ becomes a significant destination for NH_2 radicals, consistent with the sensitivity analysis (see below).

Sensitivity analyses were performed for NH_3 with different CH_4 fractions at $\varphi = 0.5$, T_c = 1000 K, P_c = 60 bar, as shown in Fig. 9(a). As observed previously [18,25], $H_2NO + O_2 = HNO + HO_2$ and $NH_2 + NO = NNH + OH$ promote ignition most in pure NH_3, and compete with $NH_2 + NO = H_2O + N_2$, as most inhibiting. At 5% CH_4, two new promoting reactions appear: $CH_4 + NH_2 = CH_3 + NH_3$ and $CH_3OO + NO = CH_3O + NO_2$. However, at 50% CH_4, $CH_4 + NH_2 = CH_3 + NH_3$ becomes slightly inhibiting. Examination of the net rates of reaction shows that this reaction proceeds in the direction as written for methane fractions in the range of 5–95%. Apparently, NH_2 is an important reactant for initiating the decomposition of CH_4 at low methane fraction, while at high methane fraction, production of relatively unreac-

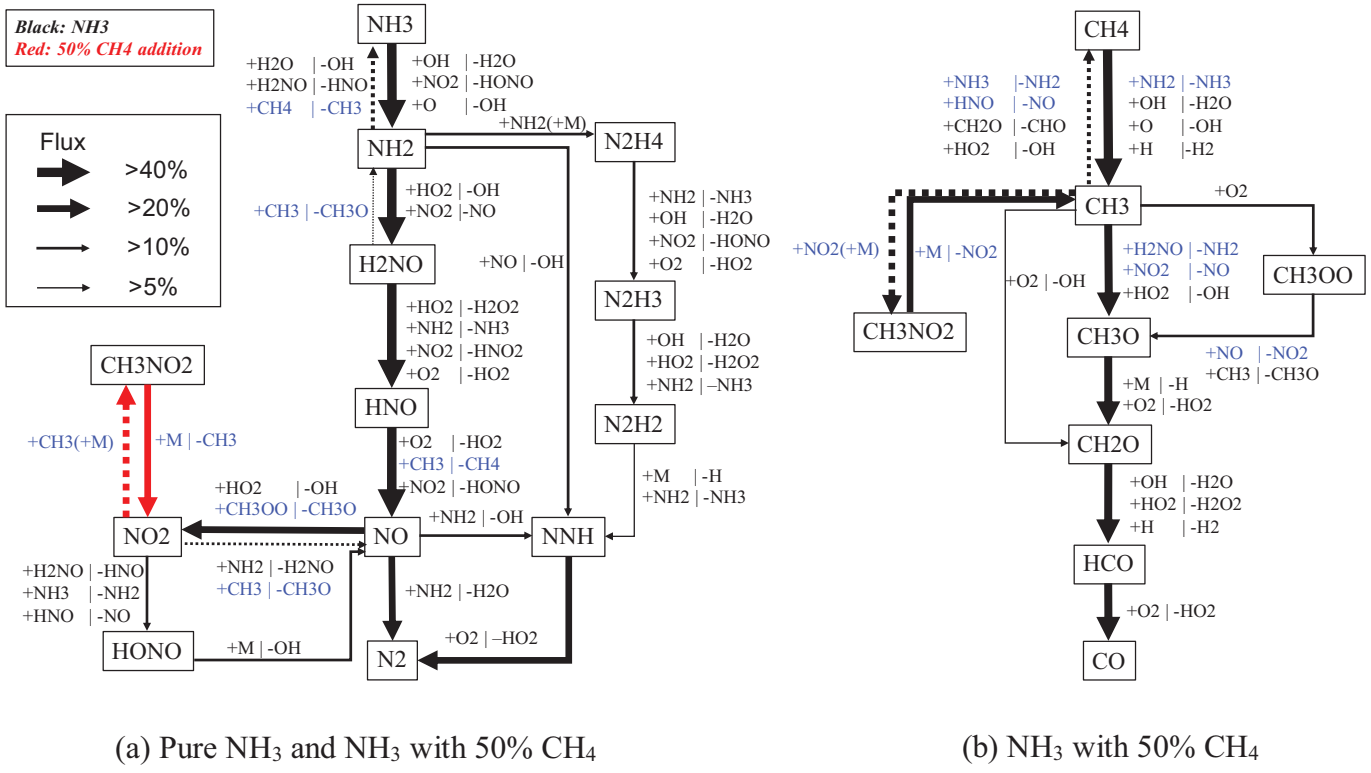

(a) Pure NH_3 and NH_3 with 50% CH_4 (b) NH_3 with 50% CH_4

Fig. 8. Flux analysis for elemental nitrogen (a) and carbon (b) showing impact of 50% CH_4 in fuel mixture at $\varphi = 0.5$, $T_c = 1000$ K, $P_c = 60$ bar, at 20% fuel consumption. In (a), black species indicate the reactants for pure NH_3, while blue species are reactants from methane oxidation. In (b), the blue species indicate reactants from NH_3 oxidation that participate in CH_4 oxidation. The red arrows in (a) indicate an additional path step coupling the N and C paths. (Fluxes lower than 5% are not shown to avoid clutter.). (For interpretation of the references to color in this figure, the reader is referred to the web version of this article.)

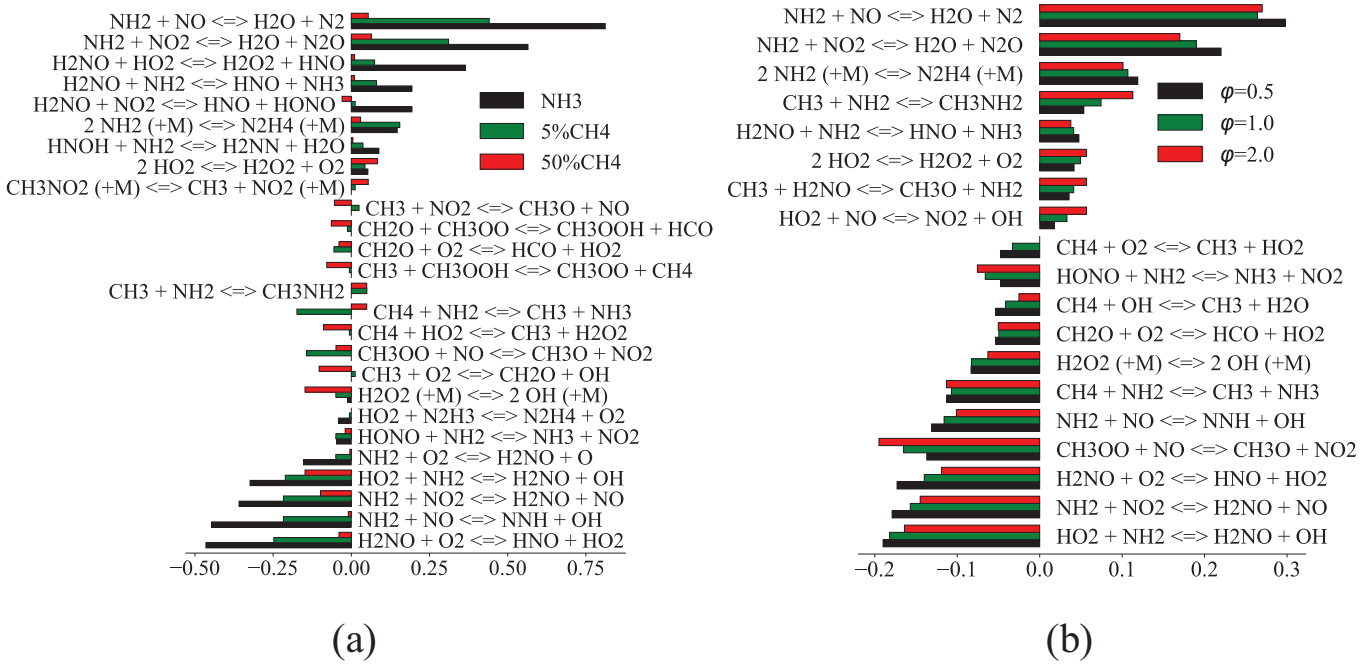

Fig. 9. Sensitivity analysis of (a) NH_3 with different CH_4 fractions at $\varphi = 0.5$, $T_c = 1000$ K, $P_c = 60$ bar and (b) NH_3 with 10% CH_4 addition at different equivalence ratios.

tive CH_3 (in terms of methane oxidation) and reconversion of NH_2 in the fuel NH_3 modestly inhibits ignition. At 50% methane, we observe a shift in the most important reactions for ignition from those among nitrogen-containing species themselves or with oxygen, as indicated above, to reactions involving H_2O_2 and HO_2, as expected in hydrocarbon ignition. Thus, the decomposition of H_2O_2 and the reaction $HO_2 + NH_2 = H_2NO + OH$ promote ignition most, while $2HO_2 = H_2O_2 + O_2$ is the most inhibiting at 50% methane. However, none of the inhibiting reactions exceeds 10% sensitivity.

To explore the effect of equivalence ratio on ignition delay times of NH_3/CH_4 mixtures, sensitivity analyses for NH_3 with 10% CH_4 addition were performed at $\varphi = 0.5$, 1.0 and 2.0, as shown

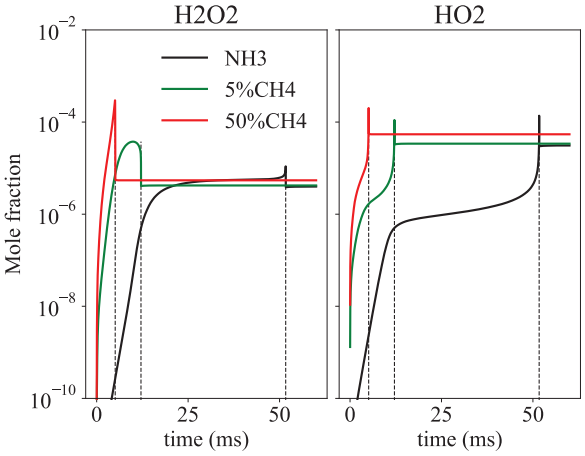

Fig. 10. Species history at different CH_4 additions at $\varphi = 0.5$, $T_c = 1000$ K, $P_c = 60$ bar. Dashed lines indicate the time of ignition.

in Fig. 9(b). Generally, variation in the equivalence ratio has a modest influence on the most sensitive reactions for NH_3 ignition with 10% CH_4 in the mixture; the most sensitive reactions are the same as those observed in Fig. 9(a) at $\varphi = 0.5$ and 5% CH_4. However, at $\varphi = 2.0$, the analysis shows that $CH_3OO + NO = CH_3O + NO_2$ has the largest promoting effect; this reaction converts the comparably unreactive peroxide to methoxy, which rapidly dissociates to yields atomic hydrogen. Since NO production is relatively limited under fuel-rich conditions, the increasing scarcity of this reactant presumably renders ignition more sensitive to this reaction and contributes to the increase in ignition delay time at this equivalence ratio seen in Fig. 6, above. The reaction $CH_3 + NH_2 = CH_3NH_2$ also gains in importance with increasing φ, resembling the recombination of methyl radicals in binding these species under richer conditions.

The sensitivity results in Fig. 9(b) also suggest a reason for the constancy of the ignition delay time with when changing from $\varphi = 0.5$ to $\varphi = 1$ shown in Fig. 6 for 10% methane in the mixture. In addition to reactions involving O_2, HO_2 and NO/NO_2, which dominate the ignition of pure ammonia, additional reactions involving CH_4 and carbon-containing species present similar sensitivity in the analysis at 10% methane. Thus, the reduction in O_2 and other oxygenated species when going from $\varphi = 0.5$ to $\varphi = 1$ slows the ignition process through reactions such as $HO_2 + NH_2 = H_2NO + OH$, but can be compensated by reactions that benefit from the increase in the methane fraction, like $CH_4 + NH_2 = CH_3 + NH_3$, facilitating ignition under these conditions.

Figure 10 illustrates the influence of CH_4 addition on the temporal profiles of some important species, at $\varphi = 0.5$, $T_c = 1000$ K, $P_c = 60$ bar, where the vertical dashed lines show the point of ignition. The largest change in species concentrations upon methane addition is on H_2O_2. As can be seen in Fig. 10, H_2O_2 is accumulated before ignition, with a maximum concentration two orders of magnitude higher at 50% CH_4 and whose growth is substantially faster than for pure NH_3. The importance of this species is further supported by ignition delay times computed for the same conditions as in Fig. 10 without H_2O_2 dissociation in the mechanism; this increases the ignition delay by a factor of 2 at 5% CH_4, increasing to a factor of 3 at 50% CH_4. Interestingly, despite its absence from the major reactions showing sensitivity for ignition in pure ammonia, H_2O_2 decomposition still has a major effect on the computed ignition delay time; removing the dissociation reaction from the mechanism increased the ignition delay for ammonia by a factor of 1.7. Together with the increasing sensitivity of ignition to H_2O_2 decomposition with increasing CH_4 fraction in the mixture, seen in Fig. 9, above, we ascribe at least part of the ignition-enhancing effect of methane addition to ammonia to its impact on H_2O_2 formation.

Given the importance of the dissociation of H_2O_2 in the ignition of all mixtures studied, we consider the rate-of-production analysis (ROP), performed at the same conditions as in Fig. 10 ($\varphi = 0.5$, $T_c = 1000$ K, $P_c = 60$ bar) for pure ammonia and 50% methane, included in the Supplemental material. We focus on the region below 1200 K, to consider the buildup of species in the pre-ignition period seen in Fig. 10. We first observe that the primary formation reaction for H_2O_2 for both pure ammonia and 50% methane is $H_2NO + HO_2 = H_2O_2 + HNO$, but with a dramatic increase in the production rate (nearly a factor of 30 at 1200 K) in the pre-ignition period for 50% methane as compared to pure ammonia. The ROP for HO_2 under the same conditions shows that the dominant reaction for the formation of HO_2 is $HNO + O_2 = HO_2 + NO$ for pure ammonia, but is augmented with $HCO + O_2 = HO_2 + CO$ and $H + O_2 + M = HO_2 + M$; furthermore, the rates of these three reactions are (each) 20–30 times higher at 50% methane than the rate of $HNO + O_2$ for pure ammonia at the same temperatures. The higher rates for these reactions result in the higher rates of H_2O_2 formation indicated above and the buildup of H_2O_2 in Fig. 10.

4. Conclusions

Autoignition delay times of NH_3/CH_4 mixtures, measured in a rapid compression machine at temperatures and pressures relevant for engines, show a strong ignition-enhancing effect of methane addition. At $\varphi = 0.5$, the ignition delay time of pure ammonia decreased by a factor of 5 at 5% methane in the mixture, decreasing by another factor of 6 upon increasing the methane fraction to 50%. The results also show that the increase in ignition delay time with increasing equivalence ratio from $\varphi = 0.5$ to $\varphi = 2$ in pure ammonia is only modestly impacted by 10% methane addition. Computed ignition delay times using six chemical mechanisms from the literature were compared with the experimental results. The comparison shows that the predictions using the mechanism by Glarborg et al. [31] as recently modified by the authors [25] reproduce the measured ignition delay times for the range of conditions studied here best, generally to within 30%.

Examination of the predicted species histories shows that the pre-ignition buildup of H_2O_2 and its precursor HO_2 are strongly enhanced, both in magnitude and rate, with increasing methane fraction in the fuel. Computed ignition delay times using the chemical mechanism excluding the dissociation of H_2O_2 increases the delay time for the mixture containing 50% methane by a factor of 3; even for pure ammonia, for which this reaction has little significance in the sensitivity analysis, the delay time increases by a factor of 1.7 upon its removal. Sensitivity and ROP analyses using this mechanism show that the important reactions responsible for shortening the ignition delay time upon methane addition shift from reactions involving nitrogen-containing species in pure ammonia to those dominating H_2O_2 and HO_2 formation at high methane fraction. Consequently, we ascribe the ignition-enhancing effect of methane addition to ammonia chiefly to its impact on the formation of H_2O_2.

Flux analysis of NH_3/CH_4 mixtures shows relatively little direct interaction between the oxidation paths of NH_3 and CH_4. The analysis indicates that $CH_4 + NH_2 = CH_3 + NH_3$ contributes substantially to the decomposition of methane early in the oxidation process, while $CH_3 + NO_2 (+M) = CH_3NO_2 (+M)$ is a significant reservoir of NO_2 at low temperature. Under fuel-rich conditions, $CH_3 + NH_2 = CH_3NH_2$ becomes a sink for NH_2 radicals.

Additionally, an anomalous pre-ignition pressure rise was observed at 50% CH_4 addition with high reproducibility, which re-

sulted in a significant shortening of the total ignition delay time, was not captured by the simulations. Given the possibility that an undesired short ignition delay time could occur in practical engines, the origins of this phenomenon are worthy of further investigation. With an eye towards practical use of ammonia/methane mixtures, future studies will combine the results presented here with those from burning velocity research to assess the utility of these mixtures in natural gas engines.

Declaration of Competing Interest

The authors declare that they have no known competing financial interests or personal relationships that could have appeared to influence the work reported in this paper.

Acknowledgments

L. Dai thanks the China Scholarship Council (CSC) for the financial support. P.G. would like to acknowledge funding from Orient's Fund.

Supplementary materials

Supplementary material associated with this article can be found, in the online version, at doi:10.1016/j.combustflame.2020.04.020.

References

[1] A. Afif, N. Radenahmad, Q. Cheok, S. Shams, J.H. Kim, A.K. Azad, Ammonia-fed fuel cells: a comprehensive review, Renew. Sustain. Energy Rev. 60 (2016) 822–835.
[2] A. Yapicioglu, I. Dincer, A review on clean ammonia as a potential fuel for power generators, Renew. Sustain. Energy Rev. 103 (2019) 96–108.
[3] G. Thomas, G. Parks, Potential Roles of Ammonia in a Hydrogen Economy: A Study of Issues Related to the use Ammonia for on-Board Vehicular Hydrogen Storage, U.S. Department of Energy, 2006, p. 23.
[4] E. Baniasadi, I. Dincer, Energy and exergy analyses of a combined ammonia-fed solid oxide fuel cell system for vehicular applications, Int. J. Hydrog. Energy. 36 (2011) 11128–11136.
[5] S. Giddey, S.P.S. Badwal, C. Munnings, M. Dolan, Ammonia as a renewable energy transportation media, ACS Sustain. Chem. Eng. 5 (2017) 10231–10239.
[6] O. Kurata, N. Iki, T. Inoue, T. Matsunuma, T. Tsujimura, H. Furutani, M. Kawano, K. Arai, E.C. Okafor, A. Hayakawa, H. Kobayashi, Development of a wide range–operable, rich-lean low-NO_x combustor for NH_3 fuel gas-turbine power generation, Proc. Combust. Inst. 37 (2019) 4587–4595.
[7] H. Kobayashi, A. Hayakawa, K.D.K.A. Somarathne, E.C. Okafor, Science and technology of ammonia combustion, Proc. Combust. Inst. 37 (2019) 109–133.
[8] A.J. Reiter, S.C. Kong, Demonstration of compression-ignition engine combustion using ammonia in reducing greenhouse gas emissions, Energy Fuels 22 (2008) 2963–2971.
[9] A.J. Reiter, S.C. Kong, Combustion and emissions characteristics of compression-ignition engine using dual ammonia-diesel fuel, Fuel 90 (2011) 87–97.
[10] K. Ryu, G.E. Zacharakis-Jutz, S.C. Kong, Performance characteristics of compression-ignition engine using high concentration of ammonia mixed with dimethyl ether, Appl. Energy 113 (2014) 488–499.
[11] O. Mathieu, E.L. Petersen, Experimental and modeling study on the high-temperature oxidation of Ammonia and related NO_x chemistry, Combust. Flame 162 (2015) 554–570.
[12] E.C. Okafor, K.D.K.A. Somarathne, A. Hayakawa, T. Kudo, O. Kurata, N. Iki, H. Kobayashi, Towards the development of an efficient low-NO_x ammonia combustor for a micro gas turbine, Proc. Combust. Inst. 37 (2019) 4597–4606.
[13] K. Takizawa, A. Takahashi, K. Tokuhashi, S. Kondo, A. Sekiya, Burning velocity measurements of nitrogen-containing compounds, J. Hazard. Mater. 155 (2008) 144–152.
[14] Y. Arakawa, R. Mimoto, T. Kudo, A. Hayakawa, H. Kobayashi, T. Goto, Laminar burning velocity and Markstein length of ammonia/air premixed flames at various pressures, Fuel 159 (2015) 98–106.
[15] P. Kumar, T.R. Meyer, Experimental and modeling study of chemical-kinetics mechanisms for H_2-NH_3-air mixtures in laminar premixed jet flames, Fuel 108 (2013) 166–176.
[16] J. Li, H. Huang, N. Kobayashi, C. Wang, H. Yuan, Numerical study on laminar burning velocity and ignition delay time of ammonia flame with hydrogen addition, Energy 126 (2017) 796–809.
[17] M. Pochet, V. Dias, B. Moreau, F. Foucher, H. Jeanmart, F. Contino, Experimental and numerical study, under LTC conditions, of ammonia ignition delay with and without hydrogen addition, Proc. Combust. Inst. 37 (2018) 621–629.
[18] X. He, B. Shu, D. Nascimento, K. Moshammer, M. Costa, R.X. Fernandes, Auto-ignition kinetics of ammonia and ammonia/hydrogen mixtures at intermediate temperatures and high pressures, Combust. Flame 206 (2019) 189–200.
[19] X. Han, Z. Wang, M. Costa, Z. Sun, Y. He, K. Cen, Experimental and kinetic modeling study of laminar burning velocities of NH_3/air, NH_3/H_2/air, NH_3/CO/air and NH_3/CH_4/air premixed flames, Combust. Flame 206 (2019) 214–226.
[20] C.W. Gross, S.C. Kong, Performance characteristics of a compression-ignition engine using direct-injection ammonia-DME mixtures, Fuel 103 (2013) 1069–1079.
[21] E.C. Okafor, Y. Naito, S. Colson, A. Ichikawa, T. Kudo, A. Hayakawa, H. Kobayashi, Measurement and modeling of the laminar burning velocity of methane-ammonia-air flames at high pressures using a reduced reaction mehcanism, Combust. Flame 204 (2019) submitted.
[22] F. Van den Schoor, F. Norman, L. Vandebroek, F. Verplaetsen, J. Berghmans, A numerical study of the influence of ammonia addition on the auto-ignition limits of methane/air mixtures, J. Hazard. Mater. 164 (2009) 1164–1170.
[23] N. Lamoureux, K. Marschallek-Watroba, P. Desgroux, J.F. Pauwels, M.D. Sylla, L. Gasnot, Measurements and modelling of nitrogen species in CH_4/O_2/N_2flames doped with NO, NH_3, or NH_3+NO, Combust. Flame 176 (2017) 48–59.
[24] B. Shu, S.K. Vallabhuni, X. He, G. Issayev, K. Moshammer, A. Farooq, R.X. Fernandes, A shock tube and modeling study on the autoignition properties of ammonia at intermediate temperatures, Proc. Combust. Inst. 37 (2019) 205–211.
[25] L. Dai, S. Gersen, P. Glarborg, H. Levinsky, A. Mokhov, Experimental and numerical analysis of the autoignition behavior of NH_3 and NH_3/H_2 mixtures at high pressure, Combust. Flame 215 (2020) 134–144.
[26] S. Gersen, M. van Essen, H. Levinsky, G. van Dijk, Characterizing gaseous fuels for their knock resistance based on the chemical and physical properties of the fuel, SAE Int. J. Fuels Lubr. 9 (2016) 1–13.
[27] Z. Tian, Y. Li, L. Zhang, P. Glarborg, F. Qi, An experimental and kinetic modeling study of premixed NH_3/CH_4/O_2/Ar flames at low pressure, Combust. Flame 156 (2009) 1413–1426.
[28] E.C. Okafor, Y. Naito, S. Colson, A. Ichikawa, T. Kudo, A. Hayakawa, H. Kobayashi, Experimental and numerical study of the laminar burning velocity of CH_4–NH_3–air premixed flames, Combust. Flame 187 (2018) 185–198.
[29] Ø. Skreiberg, P. Kilpinen, P. Glarborg, Ammonia chemistry below 1400 K under fuel-rich conditions in a flow reactor, Combust. Flame 136 (2004) 501–518.
[30] T. Mendiara, P. Glarborg, Ammonia chemistry in oxy-fuel combustion of methane, Combust. Flame 156 (2009) 1937–1949.
[31] P. Glarborg, J.A. Miller, B. Ruscic, S.J. Klippenstein, Modeling nitrogen chemistry in combustion, Prog. Energy Combust. Sci. 67 (2018) 31–68.
[32] K.P. Shrestha, L. Seidel, T. Zeuch, F. Mauss, Detailed kinetic mechanism for the oxidation of ammonia including the formation and reduction of nitrogen oxides, Energy Fuels 32 (2018) 10202–10217.
[33] U. of C. at S.D. Mechanical and Aerospace Engineering (Combustion Research), Chemical-Kinetic Mechanisms for Combustion Applications, http://web.eng.ucsd.edu/mae/groups/combustion/mechanism.html, (2014).
[34] R. Li, A.A. Konnov, G. He, F. Qin, D. Zhang, Chemical mechanism development and reduction for combustion of NH_3/H_2/CH_4 mixtures, Fuel 257 (2019) 116059.
[35] S. Gersen, A.V. Mokhov, J.H. Darmeveil, H.B. Levinsky, Ignition properties of n-butane and iso-butane in a rapid compression machine, Combust. Flame 157 (2010) 240–245.
[36] S. Gersen, A.V. Mokhov, J.H. Darmeveil, H.B. Levinsky, P. Glarborg, Ignition-promoting effect of NO_2 on methane, ethane and methane/ethane mixtures in a rapid compression machine, Proc. Combust. Inst. 33 (2011) 433–440.
[37] P. Park, J.C. Keck, Rapid Compression Machine Measurements of Ignition Delays for Primary Reference Fuels, SAE International, 1990 SAE Tech. Pap..
[38] S. Gersen, Experimental Study of the Combustion Properties of Methane/Hydrogen Mixtures Ph.D. Thesis, University of Groningen, 2007.
[39] D.G. Goodwin, H.K. Moffat, R.L. Speth, Cantera: An Object-Oriented Software Toolkit for Chemical Kinetics, Thermodynamics, and Transport Processes. Version 2.3.0, (2017).
[40] U. Burke, K.P. Somers, P. O'Toole, C.M. Zinner, N. Marquet, G. Bourque, E.L. Petersen, W.K. Metcalfe, Z. Serinyel, H.J. Curran, An ignition delay and kinetic modeling study of methane, dimethyl ether, and their mixtures at high pressures, Combust. Flame 162 (2015) 315–330.
[41] S. Gersen, N.B. Anikin, A.V. Mokhov, H.B. Levinsky, Ignition properties of methane/hydrogen mixtures in a rapid compression machine, Int. J. Hydrog. Energy 33 (2008) 1957–1964.
[42] H. Hashemi, J.M. Christensen, S. Gersen, H. Levinsky, S.J. Klippenstein, P. Glarborg, High-pressure oxidation of methane, Combust. Flame 172 (2016) 349–364.
[43] S. Gersen, H. Darmeveil, H. Levinsky, The effects of CO addition on the autoignition of H_2, CH_4 and CH_4/H_2 fuels at high pressure in an RCM, Combust. Flame 159 (2012) 3472–3475.
[44] S. Tanaka, F. Ayala, J.C. Keck, J.B. Heywood, Two-stage ignition in HCCI combustion and HCCI control by fuels and additives, Combust. Flame 132 (2003) 219–239.
[45] R.D. Büttgen, T. Raffius, G. Grünefeld, H.J. Koß, A. Heufer, High-speed imaging of the ignition of ethanol at engine relevant conditions in a rapid compression machine, Proc. Combust. Inst. 37 (2019) 1471–1478.
[46] M. Figueroa-Labastida, J. Badra, A.M. Elbaz, A. Farooq, Shock tube studies of ethanol preignition, Combust. Flame 198 (2018) 176–185.